Journal of Alloys and Compounds 878 (2021) 160382

Contents lists available at ScienceDirect

Journal of Alloys and Compounds

journal homepage: www.elsevier.com/locate/jalcom

Effects of modifier oxides in the nonlinear refractive index of niobium-borotellurite glasses

A.G. Pelosi[a], S.N.C. Santos[a], J. Dipold[a,c], M.B. Andrade[a], A.C. Hernandes[a], J.M.P. Almeida[a,b], C.R. Mendonça[a,*]

[a] São Carlos Institute of Physics, University of São Paulo, P.O. Box 369, 13560-970 São Carlos, SP, Brazil
[b] Department of Materials Engineering, São Carlos School of Engineering, University of São Paulo, Av. João Dagnone, 1100, 13563-120 São Carlos, SP, Brazil
[c] Centro de Lasers e Aplicações, Instituto de Pesquisas Energéticas e Nucleares, IPEN-CNEN/SP, 2242, A. Prof. Lineu Prestes, São Paulo, SP, Brazil

ARTICLE INFO

Article history:
Received 26 January 2021
Received in revised form 19 March 2021
Accepted 10 May 2021
Available online 16 May 2021

Keywords:
Femtosecond laser
Z-scan technique
Nonlinear refractive index
Transition metals oxide
Tellurite glass
BGO model

ABSTRACT

This work investigates the influence of transition metals oxides (Ta_2O_5 and ZrO_2) on the nonlinear refraction of niobium-borotellurite glasses prepared by melt-quenching technique. The closed-aperture Z-scan technique was used to measure the nonlinear refractive index (n_2) spectrum from 470 nm to 800 nm. Also, the BGO (Boling, Glass, and Owyoung) approach was used to model nonlinear spectra, considering the oxygens present in the sample as the major contribution to the nonlinearity. The samples' molar electronic polarizability was determined to further understanding the effect of the transition metals oxides on the optical properties. Structural analysis was performed by differential scanning calorimetry, Raman and Infrared spectroscopies. The results indicate that although the modifier oxides affect the structural units and glass polarizability, they are not enough to change the behavior of the nonlinear refractive index spectra, being the glass-matrix the main responsible for optical nonlinearity in the system studied here.

1. Introduction

Nonlinear optics play a fundamental role in the development of new photonics and optical devices. It can be applied in different areas, such as all-optical communication systems, telecommunication, integrated optics, optical limiting, among others [1–5]. In this sense, glasses are great candidates for nonlinear applications due to their properties, such as high transparency, thermal and chemical stability, besides the ability to manipulate such properties by adding chemical elements [6,7]. Among the oxide glasses, the tellurites are attractive due to their low phonon energies, high linear refractive index, and broad spectral transmittance window from visible to infrared regions, low melting points, absence of hygroscopic behavior, high value of dielectric constant and high third-order optical nonlinearities [8–11]. The origin of their high optical nonlinearities has been pointed out as the high polarizability of a lone pair of 5 s^2 orbital electrons in the Te^{4+} ions [12,13] and the high percentage of TeO_4 structural units present in the glass network [14]. Besides, efforts have been made to study elastic properties which are relevant to reveal details about the glass structure because it is associated with interatomic forces, shielding properties for radiation, e.g, Gamma-Rays shielding [15–17]. Studies about the linear optical properties of a series of tellurite-based glasses were made as well, which mainly relate the linear refractive index to molar refraction, which are correlated by the molar volume [18].

Tellurite glasses produced in their pure form are unstable and crystallize easily. Therefore, stability is achieved by adding other network formers and/or modifiers, which can be chosen from a variety of oxide compounds, including the alkaline metals, alkaline-earth metals, and transition metals oxides [19]. Moreover incorporating these compounds in the glass network leads to structural changes responsible for changing physical, thermos-mechanical and optical properties [20]. In this way, the study about the addition of transition metal oxides in tellurite-based glasses evidenced that such combination present semiconducting properties [21]. Hence, tellurite glasses have become suitable materials for photonic applications such as nonlinear optical devices, fiber optic amplifiers, upconversion lasers [22], blue converted WLEDs and self-cleanliness [23] and all-optical switching [24]. A significant amount of B_2O_3 in the TeO_2 glasses promotes thermal stability, optical transmittance and transparency [25]. On the other hand, Nb_2O_5 and Ta_2O_5 are known to increase the nonlinear optical response due to their empty D-orbital [12,13,26–28]. Lastly, the ZrO_2 modifier causes an increase in viscosity, glass transition temperature and melting

* Corresponding author.
E-mail address: crmendon@ifsc.usp.br (C.R. Mendonça).

https://doi.org/10.1016/j.jallcom.2021.160382
0925-8388/

temperature and raises the chemical and thermal stability of glass [8,29–31]. Although several studies have demonstrated the influence of glass former oxides and modifier oxides on the structure and properties of tellurite glass, their effect on nonlinear optical properties remains a subject of investigation.

Thus, in the present work, a study about the effects of modifier oxides on the nonlinear refractive index of tellurite glass, correlating with changes caused on the glass network. Niobium-borotellurite glasses codoped with Ta_2O_5 and ZrO_2 were characterized regarding their nonlinear optical properties using the Z-scan technique. The nonlinear refractive spectrum was obtained in the visible region (470–800 nm) in a femtosecond regime. Afterward, the experimental data were fitted by the Boling, Glass and Owyoung (BGO) model, assumes that the oxygen in the glass matrix gives the main contribution to the nonlinear optical response. To elucidating the structure-properties relationship on tellurite glasses, the optical nonlinearities were associated with changes caused by adding metal transitions Ta^{5+} and Zr^{2+} ions. The experimental results indicated that the optical nonlinearities are related to a cooperative effect of the high polarizability and the oxygen ions present in the tellurite matrix.

2. Experimental

The glass system studied herein can be described by the empirical equation $75TeO_2 \cdot 15B_2O_3 \cdot (10 - x - y)Nb_2O_5 \cdot xTa_2O_5 \cdot 1ZrO_2$, with x and y = 0 or 1 mol%. Therefore, the main matrix is composed by $75TeO_2$ - $15B_2O_3$ - $10Nb_2O_5$ (mol%), designated as TBN0. To evaluate the influence of modifier oxides, Nb_2O_5 was replaced by 1 Ta_2O_5 and 1 ZrO_2 (mol%), resulting in two other glass samples of composition $75TeO_2$ - $15B_2O_3$ - $9Nb_2O_5$ - $1Ta_2O_5$ (named TBN1) and $75TeO_2$ - $15B_2O_3$ - $8Nb_2O_5$ - $1Ta_2O_5$ - $1ZrO_2$ (named TBN2), in mol%. Table 1 summarizes the nominal composition of the three glasses as well as the code given for them.

Samples were prepared by a melt-quenching technique using an electricallt heated furnace open to atmosphere. High purity TeO_2 (Alfa Aesar 99%), B_2O_3 (Alfa Aesar 97.5%), Nb_2O_5 (Alfa Aesar 99.9%), Ta_2O_5 (TEP -) and ZrO_2 (Alfa Aesar 99%) were used as raw material. These chemical compounds were mixed and melted at 1000 °C in a platinum crucible and quenched into a stainless-steel mold at room temperature. Then, the samples were annealed at 350 °C for 11 h for stress removal. All compositions resulted in amorphous samples, free of inclusions and devitrification, checked by optical microscopy and x-ray diffraction. Optical polished 1.1 mm-thick samples were used for optical and Raman characterizations.

Glasses densities were measured at room temperature using Archimedes method, and the immersion liquid used was absolute ethanol. The glass transition (Tg) and crystallization (Tx) temperatures were measured by Differential Scanning Calorimetry (DSC – Model 2910 from TA Instruments) performed in synthetic air, heating rate of 10 °C/min, from room temperature up to 620 °C. The infrared absorption spectra were obtained using a Bruker – Vertex 70 spectrometer, operating at room temperature, in the range of 370 cm^{-1} to 4000 cm^{-1}, with a step of 2 cm^{-1}, and the glass samples were prepared in the form of KBr pellets. Raman spectroscopy of the samples was carried out using a confocal LabRAM micro-Raman system, using a solid-state laser with a wavelength of 532 nm (2.33 eV). A spectrophotometer (*UV-1800 Shimadzu*) was used to measure the linear absorption spectra in the range from 300 up to 800 nm.

Closed-aperture Z-scan technique [32,33] was employed to measure the nonlinear refractive index (n_2) spectra. In this technique, the sample is translated over the z-axis of a focused Gaussian beam. Due to the process of nonlinear refraction, the sample has a lens effect. In the case of positive n_2 (auto-focusing), when the sample is translated over the focal position, a variation in the beam transmission in the far-field will be observed according to its position in respect to the focus. Before the focus, the sample tends to diverge the beam, leading to a decrease in transmission. When the sample is at focus, it behaves like a thin lens; therefore, no significant beam changes occur in the far-field. After the focus, the combination between a divergent beam and induced lens tends to collimate the beam, leading to an increase in transmission. Ti:saphhire amplified lasers system (*CPA 2001*, Clark: MXR®) at 775 nm with 150 fs-pulse at 1 KHz repetition rate was used as excitation light source to pump an Optical Parametric Amplifier (OPA) (TOPAS®: Light Conversion) that provides pulses with 120 fs from 0.62 up to 2.7 eV (2000–460 nm). In order to achieve a Gaussian intensity profile was used a spatial filter in the Z-scan setup. The experimental error related to the nonlinear refractive index is 20%, being associated with the pulse intensity fluctuation and the experimental determination of pulse duration and beam waist.

Table 1
Sample codes and nominal compositions of tellurite glass systems.

Sample code	Glass composition (mol%)				
	TeO_2	B_2O_3	Nb_2O_5	Ta_2O_5	ZrO_2
TBN0	75	15	10	0	0
TBN1	75	15	9	1	0
TBN2	75	15	8	1	1

3. Results

Fig. 1 shows the DSC curves for samples TBN0, TBN1, and TBN2, in which one can observe glass characteristics temperatures, the glass transition temperature (Tg), the onset of crystallization temperature (Tx) and thermal stability against devitrification ($\Delta T = Tx - Tg$), all summarized in Table 2. A slight increase Tg can be noticed when the concentration of Nb^{5+} is reduced from the glass matrix (TBN0), and Ta^{5+} and Zr^{2+} ions are added to the glass structure (TBN1 and TBN2). The observed changes in Tg values are mainly affected by the introduction of Ta^{5+}, since the addition of Zr^{2+} does not change Tg, within the experimental error. Such behavior is related to the structural modification caused by the modifier oxides, as will be discussed later in the Raman and FTIR results. Additionally, it has been reported that the rise in the Ta^{5+} ions concentration increases the value of Tg in tellurite glasses [27].

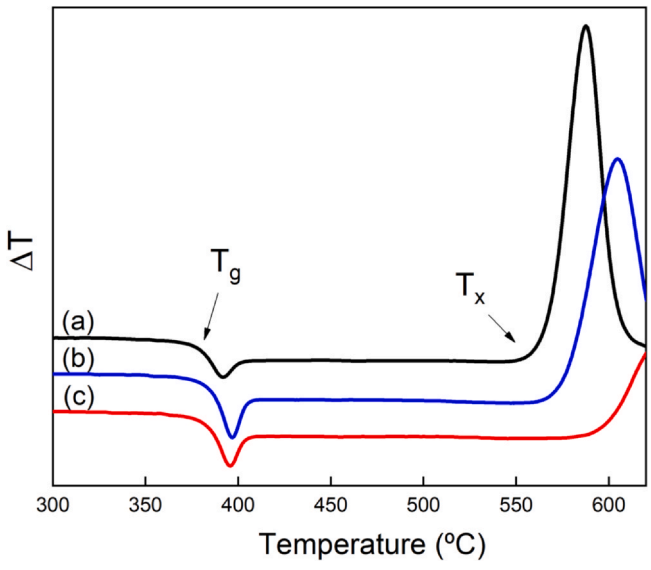

Fig. 1. DSC scans of (a) TBN0, (b) TBN1 and (c) TBN2.

Table 2
DSC thermographs of different compositions of TBN glass system.

Samples	Tg (°C)	Tx (°C)	ΔT (°C)
TBN0	377 ± 2	552 ± 2	175 ± 4
TBN1	382 ± 2	563 ± 2	181 ± 4
TBN2	381 ± 2	587 ± 2	206 ± 4

Crystallization temperature has been most significantly affected by the replacement of modifier oxides, causing an improvement of thermal stability against devitrification. In general, glasses present good thermal stability for ΔT values above 80 °C, and the samples reported herein display values at least twice higher. It is worth noting that the TBN2 sample achieved higher thermal stability due to the addition of ZrO_2 as reported in previous works [29–31].

Vibrational spectroscopy, as Raman and FTIR, are useful tools to identify and elucidate the structural units present in glass samples. The tellurite glasses have a network that consists mainly of TeO_4 units (trigonal bipyramid – tbp) [34,35], where the tellurium atom is positioned in the center of a bipyramid composed of two types of Te-O bonds. Two short bonds in equatorial position (Te-Oeq) and two long bonds in axial position (Te-Oax) [34,35] and a third axial position is occupied by the lone pair of electrons characteristic of tellurite glass [36]. The inclusion of oxide modifiers in the glass network, like transition metal oxides, can lead to the formation of TeO_{3+1} polyhedra and TeO_3 units (trigonal pyramid – tp) [12,35]. On the other hand, vitreous B_2O_3 are composed of neutral trigonal BO_3 building blocks, which progressively changes to tetrahedral BO_4 and anionic BO_3 units, upon the addition of modifiers oxides [37]. Therefore, diverse structural units can be obtained when mixing these glass forms along with modifier oxides, as one can analyze in Raman spectra of Fig. 2.

Although the replacement of Nb by Ta and Zr ions has no significant impact on Raman spectra of the niobium-borotellurite glass (Fig. 2a), they were deconvoluted into six Gaussian peaks for specific identification, as illustrated Fig. 2(b)–(d) for TBN0, TBN1 and TBN2 samples, respectively. The weak band between 245 and 271 cm^{-1} is attributed to the stretching vibrations of Te-O-B linkage [38]. The region between 453 and 455 cm^{-1} has been attributed to the symmetrical stretching and bending vibrations of the Te-O-Te bonds that share TeO_4 tbp and TeO_3 tp units [39,40]. The band between 504 and 508 cm^{-1} is assigned to the Te-O-Nb and Te-O-Te bridges [13]. The intense band in 663–665 cm^{-1} can be attributed to two possible explanations: First, the asymmetric and stretching vibrations Te-O bond of TeO_4 units [35,40]. Second, to the stretching vibration of the Nb-O bonds in Nb-O-Nb bridges [13]. The following band located in the 768–771 cm^{-1} region is ascribed to the Te-O bond's stretching vibrations in TeO_3 tp units [34,40]. The last band observed in the Raman spectrum in the region of 885–895 cm^{-1} is reported to the bending and vibration modes of the Nb-O-Nb bond and the symmetrical stretching vibrations of the Nb-O bonds, both found in the NbO_6 octahedra [26,40]. Despite little changes in Raman spectra, quantitative analyses based on the deconvoluted areas suggest the increment of Nb-O-Nb bonds in detriment of Te-O-Nb for TBN1 sample, while TBN2 remains similar to the original matrix, TBN0. It is worth note that Raman spectrum of niobium-borotellurite glass is dominated by tellurite units, and the apparent absence of BO_3 and BO_4 units is explained due to the strong polarizability of Te-O bonds [41].

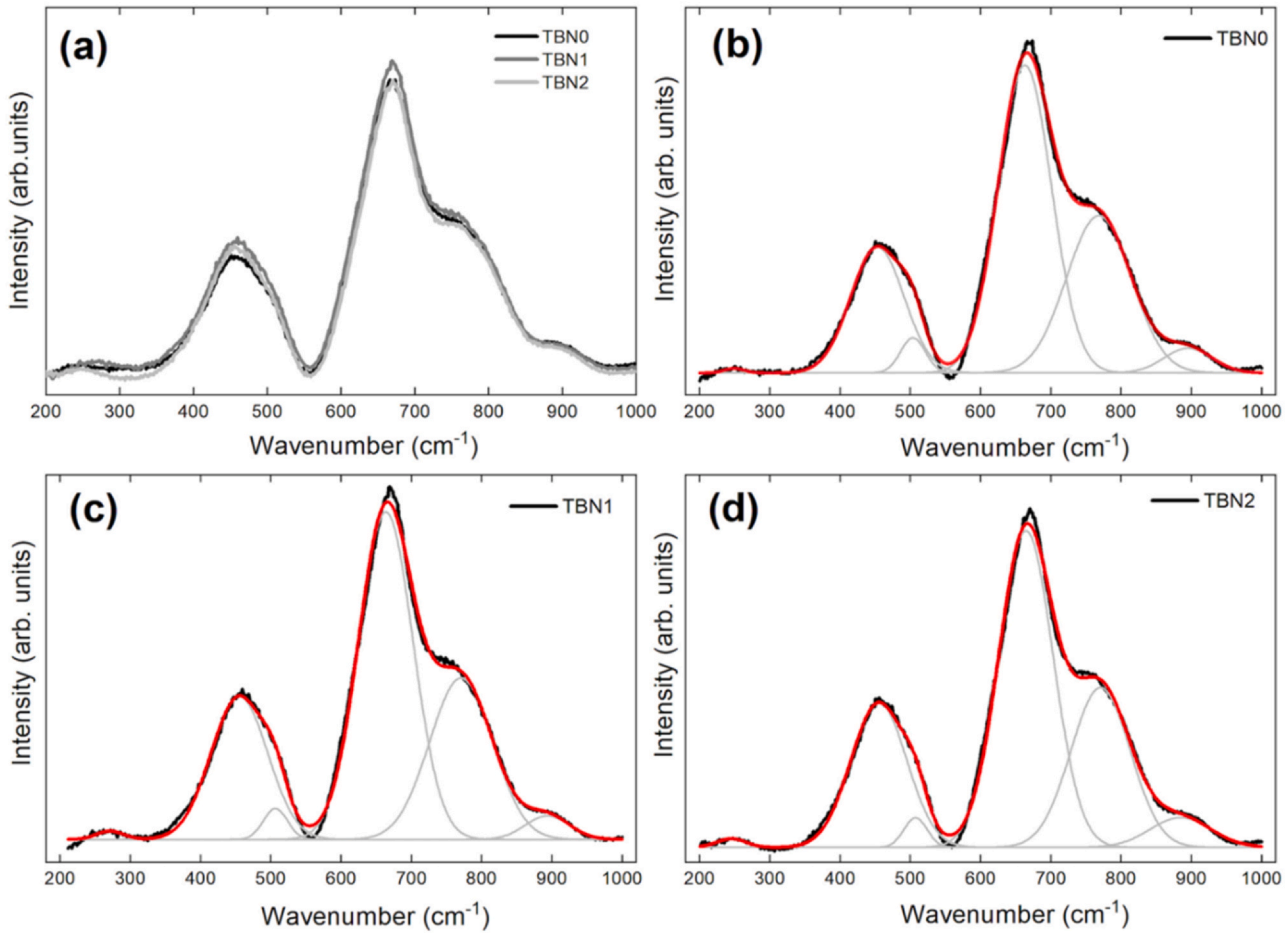

Fig. 2. Raman spectra of the samples and the deconvoluted spectra for each sample.

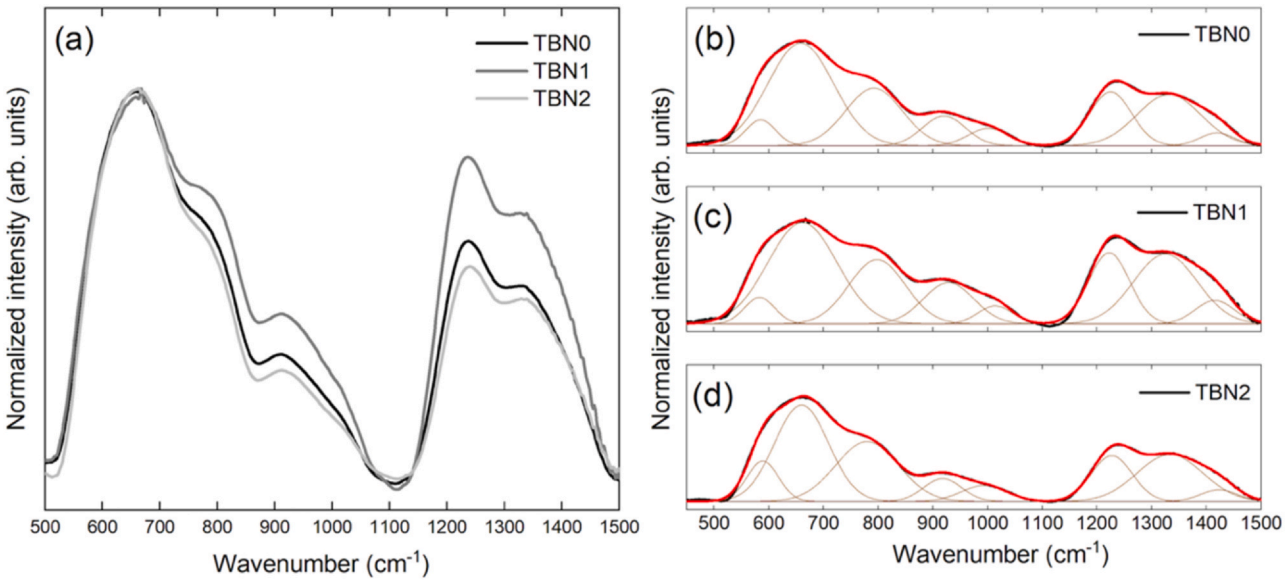

Fig. 3. (a) Infrared absorption spectra of synthesized glass compositions and deconvolution of the FTIR absorption curve for TBN0 (b), TBN1 (c) and TBN2 (d).

To investigate the influence of modifiers oxides on the borate units, FTIR measures were carried out. Fig. 3(a) shows the FTIR spectra of the samples TBN0, TBN1 and TBN2 in the range of 1500–450 cm^{-1}, which reveals various vibrational bands mainly in two regions. The first region of 450–1100 cm^{-1}, which comprises Te-O vibrations in TeO_3 and TeO_4 units and B-O stretching vibrations in BO_4 units, and the second region of 1100–1500 cm^{-1} due to B-O stretching vibrations in BO_3 units. A more detailed interpretation of the structural units can be obtained from the deconvoluted spectra using the Gaussian fitting, as shown in Fig. 3(b)–(d). In Table 3 the positions and assignments of the FTIR bands obtained from the deconvoluted spectrum are listed.

The band between 583 and 589 cm^{-1} is attributed to vibrations of Te-O-Te of TeO_4 units [42]. The intense band between 658 and 661 cm^{-1} has been attributed as the symmetric stretching vibration of the Te-O in the TeO_4 tbp units and assigned the vibration of asymmetric stretching of Te–O bonds in TeO_3 tp units [38,43–45]. In the range of 780–792 cm-1, the peak is related to the Te-O vibrations in TeO_3 tp groups [43]. In the region of 918–928 cm^{-1}, the signal can be associated with two different types of vibrations: both the stretching vibrations of Nb-O bonds in NbO_6 octahedra, and the B–O stretching vibration of BO_4 units [38,43]. The bands between 994 and 1014 cm^{-1} are ascribed to the vibration of non-bridging oxygen of BO_4 units [46].

In the regions between 1222 and 1227 cm^{-1}, 1325–1333 cm^{-1}, and 1415–1423 cm^{-1}, the bands are attributed to the stretching vibration of the bond B–O, the vibration of the bond B-O associated to vibrational modes in the borate rings and non-bridging $B–O^-$ bonds and the asymmetric stretching relaxation all of the BO_3 units, respectively [25,38,48]. The remarkable change in FTIR spectra occurs for TBN1 sample, in which a significant increase of BO_3 units (1100–1500 cm-1 region) is observed when Nb was replaced by Ta ions. Computing the relative area of tellurium based and boron-based bands, one can infer that the rising of BO_3 units is followed by the decreasing of TeO_3 units, while the TeO_4 ones remain nearly unaffected. The further replacement of Nb by Zr for TBN2 samples keeps the FTIR spectrum similar to the original matrix (TBN0), suggesting that Zr and Ta have a contrasting effect on the structural changes. It is worth noting that such structural changes support the Tg data, in which a slight increase of Tg value for TBN0 can be explained due to the increase of BO_3 units.

The linear absorption spectra of TBN0 (a), TBN1 (b) and TBN2 (c) are shown in Fig. 4, where it is clear that the samples are transparent for wavelengths longer than 450 nm, and the optical absorption edge is almost not affected by the introduction of modifier oxides, remaining close to 3.0 eV, as determined by Tauc plot method [49].

Another important optical characteristic determined was the linear refractive index (n_0), as presented in Fig. 5 all samples. The replacement of Nb ions by Ta^{5+} caused a slight decrease in the linear refractive index, but the further addition of Zr^{2+} caused an increase to values higher than the glass matrix (TBN0). The bipolar Sellmeier equation [41]:

$$n_0 = \sqrt{A + \frac{B\lambda^2}{\lambda^2 - C} + \frac{D\lambda^2}{\lambda^2 - E}} \quad (1)$$

Table 3
FTIR bands positions with corresponding band assignment.

Bands center (± 1 cm^{-1})			Band assignments
TBN0	TBN1	TBN2	
585	583	589	Vibrations of Te-O-Te in the TeO_4 units [42].
658	661	660	Symmetric stretching vibration in Te-O in tbp TeO_4 units[38–43].
			Asymmetric stretching vibration of Te-O bonds in TeO_3 tp units ([44,45].
792	798	780	Te-O vibrational modes in TeO_3 tp units [43].
920	928	918	Stretching vibrations of B-O in BO_4 units and Nb-O in NbO_6 units ([38,43]
1001	1014	994	Vibrations of non-bridging oxygen in the form of (BO_4) unit [46].
1225	1222	1227	Stretching vibrations of B-O in BO_3 units [38].
1331	1325	1333	B-O stretching vibrations in BO_3 units associated to vibrational modes in the borate rings and non-bridging $B-O^-$ bonds [47].
1419	1415	1423	Asymmetric stretching relaxation in BO_3 units [48].

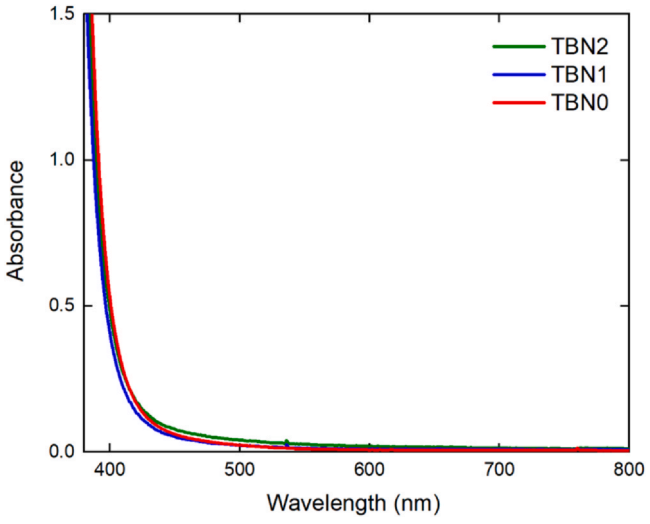

Fig. 4. Linear absorption spectrum of TBN0, TBN1 and TBN2.

was used to fit the data of Fig. 5. The solids lines in Fig. 5 display the refractive index dispersion obtained from the fitting, with the Sellmeier's coefficients (*A, B, C, D and E*) given in Table 4, with λ in micrometers. The first and second terms of the equation represent

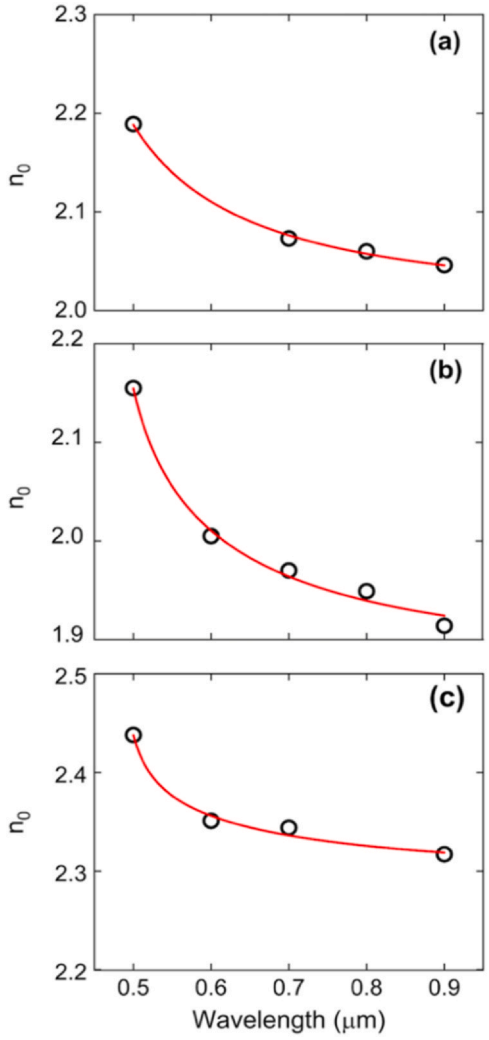

Fig. 5. Linear refractive index of TBN0 (a), TBN1 (b), and TBN2 (c). The continuous red lines represent the fitting with Sellmeier equation.

Table 4
Sellmeier coefficients for tellurite glasses obtained from the fitting shown in Fig. 5.

Sample glass	A	B	C	D	E
TBN0	2.00135	1.39542	0.01967	0.63794	0.12472
TBN1	1.9	1.5	0.0707	0.11902	0.20431
TBN2	2.24422	2.98803	0.02282	0.0482	0.22128

the contributions to refractive indices due to higher- and lower energy bandgaps of electronic absorption. The last term is related to a decrease in the refractive index due to the absorption of the network.

The nonlinear refractive index spectra for TBN0, TBN1, and TBN2 are shown in Fig. 6. Each data point in Fig. 6 corresponds to the n_2 values obtained from the closed-aperture Z-scan technique [32,33], similar to the ones presented as insets in the Figure for every sample at specific wavelengths. The nonlinear refractive spectra's behavior is approximately constant in both visible and infrared regions, except near the gap wavelength, where there is an increase of the value of the nonlinear refractive index due to the resonant enhancement of the nonlinearity. The average value of the n_2 is 0.36, 0.35 and 0.38×10^{-18} m^2/W for TNB0, TBN1 and TBN2 respectively.

In this work, the BGO [50] approach was used to model the nonlinear refractive spectra (shown in Fig. 6 as the red line). This model derives from a classical nonlinear oscillator and considers that the frequency of the incident light is far from the resonance frequency ($\omega << \omega_0$), and the second hyperpolarizability is related to the linear polarizability squared. According to the BGO model, the nonlinear refractive index, in SI (m^2/W), is given by

$$n_2(SI) = \frac{5(gs)(n_0^2+2)^2(n_0^2-1)^2}{6n_0^2 c\omega_0 \hbar(Ns)} \quad (2)$$

in which *g* is an anharmonicity parameter, *s* is the effective oscillator strength, ħ is the Planck's constant divided by 2π, *c* is the speed light, *N* is the ion's density, and n_0 is the linear refractive index at λ. One could calculate the Ns product and the resonance frequency of light ω_0 by using the following relationship:

$$\frac{4\pi(n_0^2+2)}{6(n_0^2-1)} = \frac{m(\omega_0^2-\omega^2)}{e^2(Ns)} \quad (3)$$

where *m* is the electron mass and *e* is the electron charge. By solving Eq. (3) with values of linear refractive index n_0 with their respective frequencies ω, previously obtained, one could determine the parameters ω_0 and *Ns* for each sample. Beyond that, dispersion of n_0 was used in the BGO model, represented in Eq. (2), using the Sellmeier equation (Eq. 1), with the Sellmeier's coefficients shown in Table 4.

The oscillator strength (*s*) was calculated from the ration between the density of nonlinear oscillators (*Ns*) and the density of oxygens ions in the sample (N_{ox}). One considered that oxygen plays the main role in the nonlinearities of oxide glasses [50]. The density of oxygen ions is given by

$$N_{ox} = \frac{\rho \; x \; N_A \; x \; f_{ox}}{M} \quad (4)$$

where ρ is the glass density, which is determined by Archimedes' methods, N_A is Avogadro's number, f_{ox} is the molar fraction of oxygens ions in the sample and *M* is the molecular weight of the glass. The obtained values for oxygens ions densities to TBN0, TBN1 and TBN2 were 4.6, 5.4 and 4.8×10^{22} ions/cm^3 respectively. These values were obtained using the values of linear refractive index at 500 nm for the sample TBN0, which was 2.188, and at 600 nm for samples TBN1 and TBN2, which were 2.010 and 2.356 respectively. Following the procedures described, the parameter *s* was determined for the three samples and the obtained values were 2.2, 1.8 and 2.4 for TBN0,

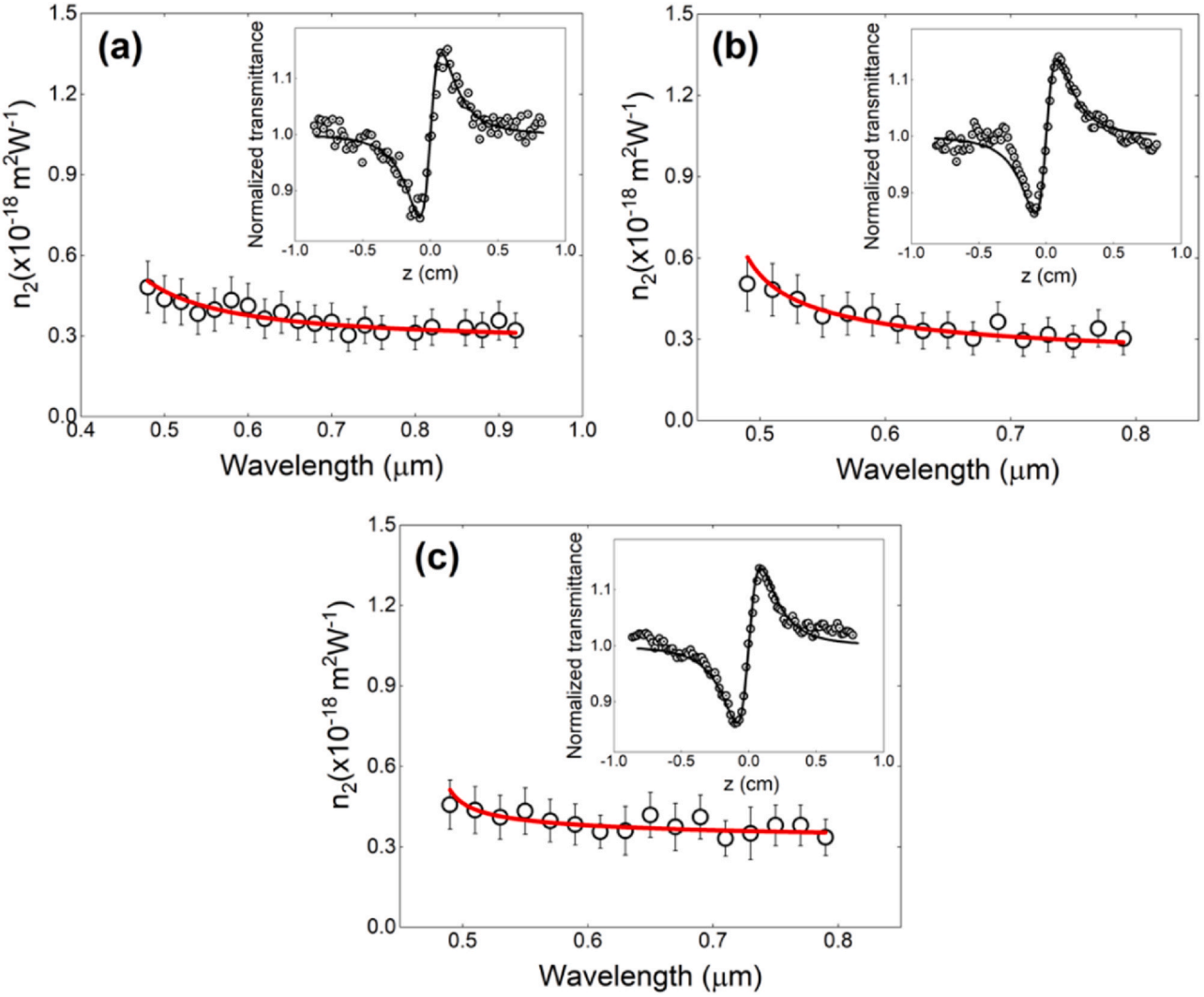

Fig. 6. Nonlinear refractive spectra (n_2) of TBN0 (a), TBN1 (b) and TBN2 (c). The red line corresponds to the fit obtained using BGO model, with parameters given in the text. The insets correspond to closed-aperture Z-scan signature obtained for each sample at 840 nm (a), 650 nm (b) and 670 nm (c).

TBN1 and TBN2 respectively. Thereby, the anharmonicity parameter *g* is the only free parameter used to fit the experimental data.

The fitting obtained employing the BGO model was represented in Fig. 6 as the red lines, from which *g* was obtained as being 0.30, 0.010 and 0.37 for TBN0, TBN1 and TBN2, respectively. Fig. 6 shows that the theoretical values of the nonlinear refractive index expected for the BGO model are in good agreement with the experimental results. The average of the nonlinear refractive index values obtained from the BGO model for all glasses studied TBN0, TBN1 and TBN2 are 0.36, 0.35 and 0.37×10^{-18} m^2/W, respectively, in which non-considerable dispersion is observed. One could notice a flat behavior of the nonlinear refractive spectra (shown in Fig. 6), therefore the glass matrix can be assigned as the main cause of the nonlinearities, presenting its major electronic transitions in the UV region of the spectrum.

Previous studies carried out thermally managed eclipse Z-scan measurements at 800 nm in TeO_2-ZnO-Na_2O glass composition co-doped with BaO, La_2O_3, or Nb_2O_5 [51]. The composition containing 5 mol% of Nb_2O_5 presented the value of n_2 of 0.35×10^{-18} m^2/W, which is of the same order of magnitude as presented in this work. Santos et al [14] also observed an increase in n_2 from about $0.29–0.35 \times 10^{-18}$ m^2/W when the concentration of Nb_2O_5 is increased from 5 mol% to 15 mol% in a TeO_2-Li_2O-Nb_2O_5 glass. These observations are in agreement with the results displayed herein, which showed high nonlinear refractive index values for glasses containing ions of transition metals, indicating that these ions also influence the increase of nonlinear optical properties of TBN glasses.

Molar electronic polarizability α_M was also determined to analyze its influence of heavy metal oxides in the optical nonlinearities. The molar electronic polarizability in ($Å^3$) is given by:

$$\alpha_M = \left(\frac{3}{4\pi N_A}\right) R_M \tag{5}$$

where R_M is the molar refraction value, given by [52,53]:

$$R_M = \left[\frac{n_0^2 - 1}{n_0^2 + 2}\right]\frac{M}{\rho} \tag{6}$$

in which n_0 is the linear refractive index, *M* is the molecular weight and ρ is density (shown in Table 5).

Table 5 depicted the values of α_M that are determined employing Eq. (5). As one could see in Fig. 7, the mean values of n_2 present an increasing tendency with the increase of α_M, which is associated to the polarizability of different transition metal oxide.

The decrease of n_2 value for TBN1 can be explained based on structural changes that showed the reduction of TeO_3 in favor of BO_3 units, which has smaller polarizability. Such structural changes, also supports the increase of Tg value for TBN1, since the B–O bond

Table 5
Molecular weight (M), density (ρ) and molar electronic polarizability (α_M) for the tellurite glasses.

Samples glass	*M* (g/mol)	ρ (g/cm^3)	α_M (Å^3)
TBN0	156.72	4.88	6.7
TBN1	158.48	4.93	6.2
TBN2	157.06	4.94	7.5

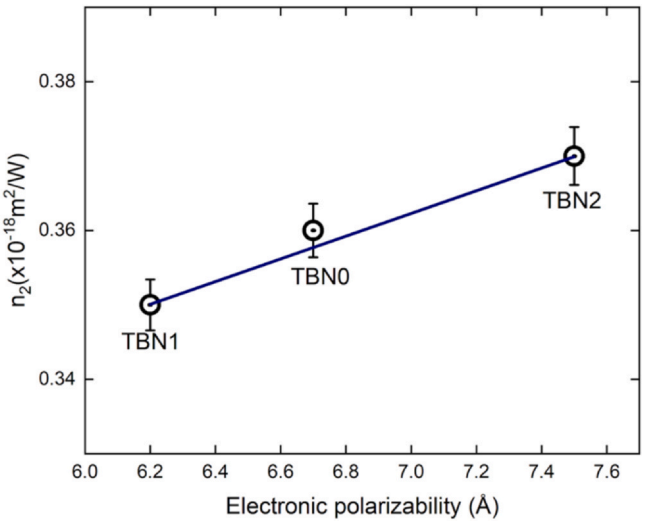

Fig. 7. Molar electronic polarizability as a function of nonlinear refractive index. The graphic shows clearly that the increase in the nonlinear refractive index depends on the addition of transition metals oxides.

energy ($E_{B\text{-}O}$ = 806.3 ± 5.0 kJ/mol) is superior than the Te-O one ($E_{Te\text{-}O}$ = 390.8 ± 8.4 kJ/mol) [37]. Particularly, the increase in the nonlinear refractive index by addition of transition metal oxides was attributed to the increment of non-bonding oxygen (from transition metal oxides), which are more polarizable. Therefore, the results presented in this work show that a combination of effects between the glass matrix and the molar electronic polarizability of transition metal oxides could contribute to the optical nonlinearities of tellurite glasses.

4. Conclusions

The role of modifier oxides in a niobium-borotellurite glass matrix (TBN0) has been investigated concerning their influence on the linear and nonlinear optical properties, correlated with the structural changes caused by Ta and Zr ions. The replacement of 1% in mol of Nb_2O_5 by 1% of Ta_2O_5 (TBN1) and the further replacement of 1% Nb_2O_5 of by 1% of ZrO_2, while keeping $1Ta_2O_5$ (TBN2) caused an increase on the characteristic temperatures (Tg and Tx) and structural changes marked by the formation of non-bridging oxygen and BO_3 units. Such structural changes affected the molar electronic polarizability, which initially decreases for the first replacement of Nb by Ta ions, followed by an increase for the second replacement of Nb by Zr ions. This same behavior was observed for the linear refractive index, that presents a dispersion of values from 2.19 to 2.05, 2.16–1.92 and 2.44–2.32 at the spectral range from 500 to 900 nm, and nonlinear refractive index, which are 0.36, 0.35 and 0.38×10^{-18} m^2/W for TBN0, TBN1 and TBN2 respectively. Both, linear and nonlinear refractive changes are related to the glass polarizability, also observed through the alteration of molar electronic polarizability, which are given by 6.7, 6.2 and 7.5 Å^3 for TBN0, TBN1 and TBN2 respectively. Such changes were not enough to affect the behavior nonlinear refractive index spectra, which are similar for all investigated samples, indicating that the niobium-borotellurite glass matrix is the main responsible for the optical nonlinearities. The experimental n_2, determined by Z-scan technique, is in agreement with the ones figured out by the BGO model. In summary, we presented an advancement in the investigation of the linear and nonlinear optical properties of tellurite glasses and the effect structural changes caused on the optical properties, particularly those associated with third-order susceptibility, contributing to the understanding of the structure-properties relationship in tellurite glass science.

CRediT authorship contribution statement

André Gasparotto Pelosi: Conceptualization, Methodology, Validation, Formal analysis, Investigation, Writing - original draft, Writing - review & editing, Visualization. **Sabrina Nicoleti Carvalho dos Santos:** Conceptualization, Methodology, Validation, Formal analysis, Investigation, Writing - original draft, Writing - review & editing, Visualization. **Jessica Dipold:** Methodology, Writing - review & editing. **Marcelo Barbosa de Andrade:** Resources, Writing - review & editing. **Antonio Carlos Hernandes:** Resources, Writing - Review & Editing. **Juliana Mara Pinto de Almeida:** Methodology, Resources, Writing - review & editing. **Cleber Renato Mendonça:** Conceptualization, Methodology, Validation, Investigation, Resources, Writing - review & editing, Visualization, Supervision, Project administration, Funding acquisition.

Declaration of Competing Interest

The authors declare that they have no known competing financial interests or personal relationships that could have appeared to influence the work reported in this paper.

Acknowledgments

The authors gratefully acknowledge Financial support from the Coordenação de Aperfeiçoamento de Pessoal de Nível Superior (CAPES) – Finance Code 001, Conselho Nacional de Desenvolvimento Científico e Tecnológico (CNPq) and Fundação de Amparo à Pesquisa do Estado de São Paulo (FAPESP) grant 2018/11283-7.

References

[1] M.V. Rao, V.V. Ravi Kanth Kumar, N.K. Shihab, D.N. Rao, Third order nonlinear and optical limiting properties of alkaline bismuth borate glasses, Opt. Laser Technol. 107 (2018) 110–115, https://doi.org/10.1016/j.optlastec.2018.05.035
[2] Z. Shi, N. Dong, D. Zhang, X. Jiang, G. Du, S. Lv, J. Chen, J. Wang, S. Zhou, Transparent niobate glass-ceramics for optical limiting, J. Am. Ceram. Soc. 102 (2019) 3965–3971, https://doi.org/10.1111/jace.16280
[3] A. Krasnok, S. Li, S. Lepeshov, R. Savelev, D.G. Baranov, A. Alú, All-optical switching and unidirectional plasmon launching with nonlinear dielectric nanoantennas, Phys. Rev. Appl. 9 (2018) 14015, https://doi.org/10.1103/PhysRevApplied.9.014015
[4] L. Wang, J. Zeng, L. Zhu, D. Yang, Q. Zhang, P. Zhang, X. Wang, S. Dai, All-optical switching in long-period fiber grating with highly nonlinear chalcogenide fibers, Appl. Opt. 57 (2018) 10044–10050, https://doi.org/10.1364/AO.57.010044
[5] G. Grinblat, R. Berté, M.P. Nielsen, Y. Li, R.F. Oulton, S.A. Maier, Sub-20 fs all-optical switching in a single Au-Clad Si nanodisk, Nano Lett. 18 (2018) 7896–7900, https://doi.org/10.1021/acs.nanolett.8b03770
[6] S. Cakmakyapan, P.K. Lu, A. Navabi, M. Jarrahi, Gold-patched graphene nanostripes for high-responsivity and ultrafast photodetection from the visible to infrared regime, Light Sci. Appl. 7 (2018) 20, https://doi.org/10.1038/s41377-018-0020-2
[7] J. Yin, Z. Tan, H. Hong, J. Wu, H. Yuan, Y. Liu, C. Chen, C. Tan, F. Yao, T. Li, Y. Chen, Z. Liu, K. Liu, H. Peng, Ultrafast and highly sensitive infrared photodetectors based on two-dimensional oxyselenide crystals, Nat. Commun. 9 (2018) 3311, https://doi.org/10.1038/s41467-018-05874-2
[8] A. Kaur, A. Khanna, C. Pesquera, F. González, V. Sathe, Preparation and characterization of lead and zinc tellurite glasses, J. Non Cryst. Solids 356 (2010) 864–872, https://doi.org/10.1016/j.jnoncrysol.2010.01.005
[9] E. Yousef, M. Hotzel, C. Rüssel, Effect of ZnO and Bi_2O_3 addition on linear and non-linear optical properties of tellurite glasses, J. Non Cryst. Solids 353 (2007) 333–338, https://doi.org/10.1016/j.jnoncrysol.2006.12.009

[10] R.N. Hampton, W. Hong, G.A. Saunders, R.A. El-Mallawany, The electrical conductivity of pure and binary TeO_2 glasses, J. Non Cryst. Solids 94 (1987) 307–314, https://doi.org/10.1016/S0022-3093(87)80066-2

[11] R.N. Hampton, W. Hong, G. Saunders, R. El-Mallawany, The dielectric-properties of tellurite glass, Eur. J. Glas. Sci. Technol. Part B Phys. Chem. Glass 29 (1988) 100–105.

[12] A.G. Kalampounias, G.N. Papatheodorou, S.N. Yannopoulos, A temperature dependence Raman study of the $0.1Nb_2O_5$-$0.9TeO_2$ glass-forming system, J. Phys. Chem. Solids 67 (2006) 725–731, https://doi.org/10.1016/j.jpcs.2005.11.001

[13] M.R. Zaki, D. Hamani, M. Dutreilh-Colas, J.-R. Duclère, J. de Clermont-Gallerande, T. Hayakawa, O. Masson, P. Thomas, Structural investigation of new tellurite glasses belonging to the TeO_2-$NbO_{2.5}$-WO_3 system, and a study of their linear and nonlinear optical properties, J. Non Cryst. Solids 512 (2019) 161–173, https://doi.org/10.1016/j.jnoncrysol.2019.02.027

[14] F.A. Santos, M.S. Figueiredo, E.C. Barbano, L. Misoguti, S.M. Lima, L.H.C. Andrade, K. Yukimitu, J.C.S. Moraes, Influence of lattice modifier on the nonlinear refractive index of tellurite glass, Ceram. Int. 43 (2017) 15201–15204, https://doi.org/10.1016/j.ceramint.2017.08.054

[15] R. El-Mallawany, Longitudinal elastic constants of tellurite glasses, J. Appl. Phys. 73 (1993) 4878–4880, https://doi.org/10.1063/1.353804

[16] R. El-Mallawany, M. Sidkey, A. Khafagy, H. Afifi, Elastic constants of semiconducting tellurite glasses, Mater. Chem. Phys. 37 (1994) 295–298, https://doi.org/10.1016/0254-0584(94)90167-8

[17] M.I. Sayyed, R. El-Mallawany, Shielding properties of $(100\text{-}x)TeO_2$–$(x)MoO_3$ glasses, Mater. Chem. Phys. 201 (2017) 50–56, https://doi.org/10.1016/j.matchemphys.2017.08.035

[18] R. El-Mallawany, The optical properties of tellurite glasses, J. Appl. Phys. 72 (1992) 1774–1777, https://doi.org/10.1063/1.351649

[19] A. Šantić, A. Moguš-Milanković, K. Furić, M. Rajić-Linarić, C.S. Ray, D.E. Day, Structural properties and crystallization of sodium tellurite glasses, Croat. Chem. Acta 81 (2008) 559–567.

[20] H. Desirena, A. Schülzgen, S. Sabet, G. Ramos-Ortiz, E. de la Rosa, N. Peyghambarian, Effect of alkali metal oxides R_2O (R = Li, Na, K, Rb and Cs) and network intermediate MO (M = Zn, Mg, Ba and Pb) in tellurite glasses, Opt. Mater. 31 (2009) 784–789, https://doi.org/10.1016/j.optmat.2008.08.005

[21] R. El-Mallawany, Devitrification and vitrification of tellurite glasses, J. Mater. Sci. Mater. Electron. 6 (1995) 1–3, https://doi.org/10.1007/BF00208125

[22] V. Kumar Rai, S.B. Rai, Optical transitions of Dy_{3+} in tellurite glass: observation of upconversion, Solid State Commun. 132 (2004) 647–652, https://doi.org/10.1016/j.ssc.2004.07.067

[23] S.H. Elazoumi, H.A.A. Sidek, Y.S. Rammah, R. El-Mallawany, M.K. Halimah, K.A. Matori, M.H.M. Zaid, Effect of PbO on optical properties of tellurite glass, Results Phys. 8 (2018) 16–25, https://doi.org/10.1016/j.rinp.2017.11.010

[24] M.E. Lines, Oxide glasses for fast photonic switching: a comparative study, J. Appl. Phys. 69 (1991) 6876–6884, https://doi.org/10.1063/1.347677

[25] G. Kilic, Role of Nd^{3+} ions in TeO_2–V_2O_5–(B_2O_3/Nd_2O_3) glasses: structural, optical, and thermal characterization, J. Mater. Sci. Mater. Electron. 31 (2020) 12892–12902, https://doi.org/10.1007/s10854-020-03842-5

[26] T. Hayakawa, M. Hayakawa, M. Nogami, P. Thomas, Nonlinear optical properties and glass structure for MO–Nb_2O_5–TeO_2 (M=Zn, Mg, Ca, Sr, Ba) glasses, Opt. Mater. 32 (2010) 448–455, https://doi.org/10.1016/j.optmat.2009.10.006

[27] G. Guery, A. Fargues, T. Cardinal, M. Dussauze, F. Adamietz, V. Rodriguez, J.D. Musgraves, K. Richardson, P. Thomas, Impact of tellurite-based glass structure on Raman gain, Chem. Phys. Lett. 554 (2012) 123–127, https://doi.org/10.1016/j.cplett.2012.10.023

[28] S.-H. Kim, T. Yoko, Nonlinear optical properties of TeO_2-based glasses: MOx-TeO_2 (M = Sc, Ti, V, Nb, Mo, Ta, and W) binary glasses, J. Am. Ceram. Soc. 78 (1995) 1061–1065, https://doi.org/10.1111/j.1151-2916.1995.tb08437.x

[29] R. Karell, M. Chromčíková, M. Liška, Properties of selected zirconia containing silicate glasses III, J. Ceram. 52 (2008) 102–108.

[30] S. Khan, G. Kaur, K. Singh, Effect of ZrO_2 on dielectric, optical and structural properties of yttrium calcium borosilicate glasses, Ceram. Int. 43 (2017) 722–727, https://doi.org/10.1016/j.ceramint.2016.09.219

[31] K.V. Krishnaiah, P. Venkatalakshmamma, C. Basavapoornima, I.R. Martín, K. Soler-Carracedo, M.A. Hernández-Rodríguez, V. Venkatramu, C.K. Jayasankar, Er^{3+}-doped tellurite glasses for enhancing a solar cell photocurrent through photon upconversion upon 1500 nm excitation, Mater. Chem. Phys. 199 (2017) 67–72, https://doi.org/10.1016/j.matchemphys.2017.06.003

[32] M. Sheik-bahae, A.A. Said, E.W. Van Stryland, High-sensitivity, single-beam n_2 measurements, Opt. Lett. 14 (1989) 955–957, https://doi.org/10.1364/OL.14.000955

[33] M. Sheik-Bahae, A.A. Said, T.-. Wei, D.J. Hagan, E.W. Van Stryland, Sensitive measurement of optical nonlinearities using a single beam, IEEE J. Quantum Electron. 26 (1990) 760–769, https://doi.org/10.1109/3.53394

[34] S. Chakraborty, L.H. Singh, G.K. Sharma, T.R. Ravindran, Understanding alkali oxide induced structural modification at different length-scales in tellurite glasses for improved optical properties, J. Alloy. Compd. 853 (2021) 156990, https://doi.org/10.1016/j.jallcom.2020.156990

[35] I. Grelowska, M. Reben, B. Burtan, M. Sitarz, J. Cisowski, E.S. Yousef, A. Knapik, M. Dudek, Structural and optical study of tellurite–barium glasses, J. Mol. Struct. 1126 (2016) 219–225, https://doi.org/10.1016/j.molstruc.2016.01.034

[36] M.A.T. Marple, M. Jesuit, I. Hung, Z. Gan, S. Feller, S. Sen, Structure of TeO_2 glass: results from $2D^{125}Te$ NMR spectroscopy, J. Non Cryst. Solids 513 (2019) 183–190, https://doi.org/10.1016/j.jnoncrysol.2019.03.019

[37] K.I. Chatzipanagis, N.S. Tagiara, D. Möncke, S. Kundu, A.C.M. Rodrigues, E.I. Kamitsos, Vibrational study of lithium borotellurite glasses, J. Non Cryst. Solids 540 (2020) 120011, https://doi.org/10.1016/j.jnoncrysol.2020.120011

[38] G. Swapna, M. Upender, Raman Prasad, FTIR, thermal and optical properties of TeO_2-Nb_2O_5-B_2O_3-V_2O_5 quaternary glass system, J. Taibah Univ. Sci. 11 (2017) 583–592, https://doi.org/10.1016/j.jtusci.2016.02.008

[39] H. Fares, I. Jlassi, H. Elhouichet, M. Férid, Investigations of thermal, structural and optical properties of tellurite glass with WO_3 adding, J. Non Cryst. Solids 396–397 (2014) 1–7, https://doi.org/10.1016/j.jnoncrysol.2014.04.012

[40] A. Kaur, A. Khanna, V.G. Sathe, F. Gonzalez, B. Ortiz, Optical, thermal, and structural properties of Nb_2O_5-TeO_2 and WO_3-TeO_2 glasses, Phase Transit. 86 (2013) 598–619, https://doi.org/10.1080/01411594.2012.727998

[41] S.N.C. Santos, K.T. Paula, J.M.P. Almeida, A.C. Hernandes, C.R. Mendonça, Effect of Tb^{3+}/Yb^{3+} in the nonlinear refractive spectrum of CaLiBO glasses, J. Non Cryst. Solids 524 (2019) 119637, https://doi.org/10.1016/j.jnoncrysol.2019.119637

[42] U.G. Işsever, G. Kilic, M. Peker, T. Ünaldi, A.Ş. Aybek, Effect of low ratio V^{5+} doping on structural and optical properties of borotellurite semiconducting oxide glasses, J. Mater. Sci. Mater. Electron. 30 (2019) 15156–15167, https://doi.org/10.1007/s10854-019-01889-7

[43] N. Elkhoshkhany, M.A. Khatab, M.A. Kabary, Thermal, FTIR and UV spectral studies on tellurite glasses doped with cerium oxide, Ceram. Int. 44 (2018) 2789–2796, https://doi.org/10.1016/j.ceramint.2017.11.019

[44] J.V. Gunha, A. Gonçalves, A. Somer, A.V.C. de Andrade, D.T. Dias, A. Novatski, Thermal, structural and optical properties of TeO_2–Na_2O–TiO_2 glassy system, J. Mater. Sci. Mater. Electron. 30 (2019) 16695–16701, https://doi.org/10.1007/s10854-019-01496-6

[45] G. Lakshminarayana, K.M. Kaky, S.O. Baki, A. Lira, P. Nayar, I.V. Kityk, M.A. Mahdi, Physical, structural, thermal, and optical spectroscopy studies of TeO_2–B_2O_3–MoO_3–ZnO–R_2O (R = Li, Na, and K)/MO (M = Mg, Ca, and Pb) glasses, J. Alloy. Compd. 690 (2017) 799–816, https://doi.org/10.1016/j.jallcom.2016.08.180

[46] A. Azuraida, M.K. Halimah, A.A. Sidek, C.A.C. Azurahanim, S.M. Iskandar, M. Ishak, A. Nurazlin, Comparative studies of bismuth and barium boro-tellurite glass system: Structural and optical properties, Chalcogenide Lett. 12 (2015) 497–503.

[47] S. Rada, V. Dan, M. Rada, E. Culea, Gadolinium-environment in borate-tellurate glass ceramics studied by FTIR and EPR spectroscopy, J. Non Cryst. Solids 356 (2010) 474–479, https://doi.org/10.1016/j.jnoncrysol.2009.12.011

[48] A. Ichoja, S. Hashim, S.K. Ghoshal, I.H. Hashim, R.S. Omar, Physical, structural and optical studies on magnesium borate glasses doped with dysprosium ion, J. Rare Earths 36 (2018) 1264–1271, https://doi.org/10.1016/j.jre.2018.05.013

[49] J. Tauc, Optical properties and electronic structure of amorphous Ge and Si, Mater. Res. Bull. 3 (1968) 37–46, https://doi.org/10.1016/0025-5408(68)90023-8

[50] N.L. Boling, A.J. Glass, A. Owyoung, Empirical relationships for predicting nonlinear refractive index changes in optical solids, IEEE J. Quantum Electron. (1978), https://doi.org/10.1109/JQE.1978.1069847

[51] F.E.P. dos Santos, F.C. Fávero, A.S.L. Gomes, J. Xing, Q. Chen, M. Fokine, I.C.S. Carvalho, Evaluation of the third-order nonlinear optical properties of tellurite glasses by thermally managed eclipse Z-scan, J. Appl. Phys. 105 (2009) 24512, https://doi.org/10.1063/1.3072630

[52] R.R. Reddy, Y. Nazeer Ahammed, P. Abdul Azeem, K. Rama Gopal, T.V.R. Rao, Electronic polarizability and optical basicity properties of oxide glasses through average electronegativity, J. Non Cryst. Solids 286 (2001) 169–180, https://doi.org/10.1016/S0022-3093(01)00481-1

[53] Y.B. Saddeek, K. Aly, G. Abbady, N. Afify, K.H.S. Shaaban, A. Dahshan, Optical and structural evaluation of bismuth alumina-borate glasses doped with different amounts of (Y_2O_3), J. Non Cryst. Solids 454 (2016) 13–18, https://doi.org/10.1016/j.jnoncrysol.2016.10.023